

## UNIFIED METHODS FOR COMPUTING COMPRESSIBLE AND INCOMPRESSIBLE FLOWS

P. Wesseling, D.R. van der Heul<sup>1</sup>, and C. Vuik

J.M. Burgers Center and Delft University of Technology  
Faculty of Information Technology and Systems  
Mekelweg 4, 2628 CD Delft, The Netherlands  
e-mail: P.Wesseling@its.tudelft.nl, web page:  
<http://dutita0.twi.tudelft.nl/people/P.Wesseling.html>

**Key words:** computational fluid dynamics, compressible flow, incompressible flow, finite volume method, cavitation, nonconvex hyperbolic systems.

**Abstract.** *To develop unified computing methods that are accurate and efficient both for compressible and incompressible flows, one may modify methods developed for the fully compressible case, or, vice-versa, modify incompressible methods. Both approaches are reviewed. One leads to colocated, the other to staggered schemes. The latter resemble closely classical schemes for the hyperbolic systems of equations governing atmospheric and oceanographic flows. General equations of state are considered, leading to nonconvex hyperbolic systems. A simple way to solve a class of Riemann problems is presented, using Oleinik's formulation of the entropy condition. The Osher scheme and a staggered scheme are found to converge with the same accuracy to the physical weak solution. The staggered scheme turns out to be useful for computing with the homogeneous equilibrium model a hydrodynamic flow with cavitation, in which a region where the Mach number reaches 25 is embedded in a domain where the Mach number equals  $10^{-3}$ .*

---

<sup>1</sup>Supported by the Netherlands Organization for Scientific Research (NWO)

## 1 INTRODUCTION

If there are regions in the flow domain where the Mach number  $M$  is not small, the compressible equations of the motion must be used. Although these are uniformly valid for  $M \geq 0$  (until real gas effects set in), standard numerical methods for the compressible case break down when  $M \lesssim 0.2$ , as discussed below. Therefore different methods, that are uniformly valid for  $M \geq 0$ , are required if regions with  $M \lesssim 0.2$  and  $M \gtrsim 0.2$  occur simultaneously. These what we will call unified methods are the subject of this paper.

Typical circumstances where  $M$  is small in parts of the domain but where compressibility cannot be neglected are the following. Due to the geometry of the domain, local high Mach zones may be embedded in a low Mach flow. Examples are the flow in the inlet of an internal combustion engine, or hydrodynamic flow with cavitation using the homogeneous equilibrium model, discussed below. Conversely, during the hyperbolic flight phase of a re-entering space vehicle, thick boundary layers and separation zones develop, in which  $M \lesssim 0.2$ .

First, we will explain why standard computing methods for compressible flow break down as  $M \downarrow 0$ . Then we will discuss the concept of preconditioning, by which methods for compressible flow may be extended to the low Mach number regime. Finally, we will discuss generalization of methods for incompressible flow to the compressible case.

## 2 DIFFICULTIES WITH THE ZERO MACH NUMBER LIMIT

It suffices to consider the one-dimensional Euler equations, in the usual notation:

$$U_t + f(U)_x = 0, \quad U = \begin{pmatrix} \rho \\ m \\ \rho E \end{pmatrix}, \quad f = \begin{pmatrix} m \\ m^2/\rho + p(\rho, T) \\ m + 1 \end{pmatrix}. \quad (1)$$

Assuming a perfect gas, we have  $p = \rho RT$ . The following well-known considerations show that numerical difficulties are to be expected when  $M \downarrow 0$ , which  $M = u/c$ ,  $u = m/\rho$ , and the speed of sound given by  $c = \sqrt{\gamma p/\rho}$ .

The eigenvalues of the Jacobian  $f'(U)$  are given by  $\lambda_1 = u - c$ ,  $\lambda_2 = u$ ,  $\lambda_3 = u + c$ . The spectral number of  $f'$  is defined by  $\kappa(f') = \rho(f')\rho((f')^{-1})$ , with  $\rho$  the spectral radius. For simplicity we assume  $u \geq 0$ . Then

$$\kappa(f') = (u + c) \max\left\{\frac{1}{u}, \frac{1}{|u - c|}\right\} = \max\left\{1 + \frac{1}{M}, \frac{M + 1}{|M - 1|}\right\}.$$

When  $\kappa(f') \gg 1$ ,  $f'$  is ill-conditioned, and numerical difficulties may crop up. This is seen to occur in the sonic limit  $M \rightarrow 1$  and the incompressible limit  $M \downarrow 0$ . In standard computing methods for compressible flow a carefully designed artificial viscosity term is incorporated, either implicitly as in approximate Riemann solvers or flux-splitting methods (e.g. [35], [29], [49], [23], or explicitly, as in the Jameson-Schmidt-Turkel scheme ([16]). This takes care of the singularity at  $M = 1$ , but nothing is done about the

singularity at  $M = 0$ , and in practice these schemes are inapplicable when large regions with  $M \lesssim 0$  occur. For more information about the underlying causes for this, see [19], [9].

Another indication of trouble is stiffness of the equations. A typical stability condition for explicit schemes is  $\tau \leq h(u + c)$ , with  $\tau$  the time step and  $h$  the mesh size. In the absence of acoustic effects, the physical time scale in low Mach flow is  $L/u$ , and a reasonable time step is  $\tau_p = h/u$ . We find  $\tau/\tau_p \leq M/(1 + M)$ , so that for stability  $\tau$  must be much smaller than  $\tau_p$  if  $M \ll 1$ . When this happens a system is called stiff. Numerical inefficiency results, caused by the unwanted requirement to resolve acoustic modes, which travel with speed  $u \pm c$ .

There is also an accuracy problem. When the stiff system is solved with the required very large number of time steps, often wrong results are obtained for  $M$  small. This is shown and analyzed in [9], [42].

### 3 PRECONDITIONING

One way to alleviate the stiffness problem is to change the governing equations. This looks like putting an end to the disease by killing the patient, but is not as bad as it seems. The procedure is called preconditioning. This solves both the stiffness and the accuracy problem, as shown in [9], [42]. A practical advantage of preconditioning is that existing codes for compressible flow can be modified to improve performance for weakly compressible flow.

The principle will be explained for the one-dimensional inviscid case. Preconditioning consists of multiplication of the time-derivative by a matrix  $P^{-1}$ :

$$P^{-1}U_t + f(U)_x = 0. \quad (2)$$

Stationary solution are not affected by preconditioning, but time accuracy is lost. The preconditioning matrix  $P(U)$  is to be chosen such that (2) is less stiff than the original system as  $M \downarrow 0$ . The eigenvalues  $\lambda(Pf')$  should remain closer together than  $\lambda(f')$  as  $M \downarrow 0$ . The design of  $P(U)$  has been and still is the subject of much research. We will discuss the preconditioner proposer in [51]. We switch to new primitive variables  $Q = (p, u, T)$ , with  $T$  the temperature. The preconditioned system is

$$\Gamma Q_t + f(Q)_x = 0, \quad \Gamma = \begin{pmatrix} \theta & 0 & \rho T \\ \theta u & \rho & u\rho T \\ \theta H - 1 & \rho u & H\rho T + c_p\rho \end{pmatrix}, \quad (3)$$

where  $\theta$  is a parameter chosen as follows:

$$\theta = 1/w^2 - \rho T/(c_p\rho),$$

with  $w$  a velocity magnitude given by

$$w = \begin{cases} \varepsilon c & \text{if } |u| \leq \varepsilon c, \\ |u| & \text{if } \varepsilon c < |u| \leq c, \\ c & \text{if } |u| > c. \end{cases}$$

The parameter  $\varepsilon$  ( $\sim 10^{-5}$ ) is included to prevent singularity for  $u = 0$ . For the eigenvalues we find

$$\begin{aligned} \lambda(\Gamma^{-1} f'(Q)) &= \{u, \tilde{u} + \tilde{c}, \tilde{u} - \tilde{c}\}, \quad \tilde{u} = u(1 - \alpha), \\ \tilde{c} &= \sqrt{\alpha^2 u^2 + w^2}, \quad \alpha = (1 - \beta w^2)/2, \quad \beta = (\rho_p + \frac{\rho T}{c_p \rho}). \end{aligned}$$

For a perfect gas,  $\beta = 1/c^2$ , so that  $\alpha = (1 - M_w^2)/2$ ,  $M_w = w/c$ . Hence, when  $M = |u|/c > 1$  we have  $\alpha = 0$ , and the eigenvalues equal those of the unpreconditioned system. At low Mach we have  $\alpha \cong 1/2$ , and  $\tilde{u} \pm \tilde{c} \cong \frac{1}{2}u(1 \pm \sqrt{5})$ , so that the stiffness has been removed.

Equation (3) is discretized in space as follows. Finite volume integration gives

$$h_j \Gamma_j \frac{dQ_j}{dt} + F(Q)|_{j-1/2}^{j+1/2} = 0, \quad (4)$$

where  $h_j$  is the size of the finite volume. The Roe scheme gives

$$F_{j+1/2} = \frac{1}{2}\{f(Q_j) + f(Q_{j+1})\} - \frac{1}{2}|f'|_{j+1/2}(Q_{j+1} - Q_j).$$

Practical experience and the analysis of [9], [42] shows that this gives unsatisfactory results for  $M \lesssim 0.2$ . Much better results are obtained if the preconditioning is allowed to influence the artificial dissipation term, as follows:

$$F_{j+1/2} = \frac{1}{2}\{f(Q_j) + f(Q_{j+1})\} - \frac{1}{2}\Gamma_{j+1/2}|\Gamma^{-1}f'|_{j+1/2}(Q_{j+1} - Q_j). \quad (5)$$

For extension of this method to the two-dimensional viscous case, see [51], where successful applications to fully and weakly incompressible flows are shown.

To compute nonstationary flow, time accuracy has to be restored. This may be done by dual time stepping, introducing a pseudo-time  $s$ . Equation (4) is replaced by

$$h_j \frac{dU_j}{dt} + h_j \Gamma_j \frac{dQ_j}{dt} + F(Q)|_{j-1/2}^{j+1/2} = 0.$$

For simplicity, we choose the implicit Euler scheme in time and the explicit Euler scheme in pseudo-time, and obtain:

$$\frac{h_j}{\tau} \left( \frac{\partial U}{\partial Q} \right)_j^{m-1} (Q_j^m - Q_j^n) + \frac{h_j \Gamma_j}{\sigma} (Q_j^m - Q_j^{m-1}) + F(Q^{m-1})|_{j-1/2}^{j+1/2} = 0,$$

where  $\tau$  is the time step and  $\sigma$  the pseudo-time step. The superscript  $n$  counts physical time steps and the superscript  $m$  counts pseudo-time steps. For  $m = 0$  we put  $Q^m = Q^n$ . A time step is executed by stepping in pseudo-time with  $m = 1, 2, \dots, \bar{m}$ , where  $\bar{m}$  follows from the condition that the pseudo-time difference has become negligible, so that we have completed a time step for (4). In [51] it is shown that dual time stepping is significantly more efficient than physical time stepping if  $M \lesssim 0.2$ . Nevertheless, dual time stepping is expensive, because a large number of pseudo-time steps is required for each physical time step. As a consequence, the efficiency is much less than that of incompressible flow solvers, so that preconditioned dual time stepping methods cannot be called efficient for weakly compressible nonstationary flows. In [9] it is shown that pseudo-time stepping can be dispensed with. We can solve directly

$$\frac{dU_j}{dt} + F(Q)|_{j-1/2}^{j+1/2} = 0 ,$$

with  $F(Q)$  given by (5). As remarked in [30], for efficiency an implicit time stepping scheme must be used. If this is necessary anyway, because of a large disparity in mesh sizes for example, this is no disadvantage. However, the resulting nonlinear algebraic system is difficult, and iterative methods that have been used until now require much computing time. This still needs improvement.

Considering extensions to more dimensions, the viscous case, flows with combustion and chemistry and implementation of boundary conditions, we give a few pointers to the literature. For a review of early literature, see [41]. The preconditioner of [51] described above is an extension of the one introduced in [3], [4]. Iterative methods for implicit preconditioned schemes are analysed in [19], [18], [5]. Some recent publications are: [43], [8], [9].

Preconditioning is a way to extend the functionality of existing codes for fully compressible flows to almost incompressible flows. The efficiency of methods for incompressible is not matched. In the next sections the reverse route is followed, namely extension of methods for incompressible flows to compressible flows.

#### 4 MACH-UNIFORM DIMENSIONLESS EULER EQUATIONS

To get more mathematical insight in what happens as  $M \downarrow 0$  we make the governing equations dimensionless. The influence of the choice of units is conveniently shown for the following nonconservative form of (1):

$$\rho_t + m_x = 0 , \quad m_t + (um + p)_x = 0 , \quad p_t + \gamma pu_x + up_x = 0 . \quad (6)$$

The units of length, velocity, time, density and pressure are  $x_r$ ,  $u_r$ ,  $x_r/u_r$ ,  $\rho_r$  and  $p_r$ . We let  $x_r$  be a characteristic dimension of the domain and  $u_r$  a typical velocity magnitude, such as the velocity at infinity if we have flow around a body. This choice of units reflects that we are not interested in acoustics, for which the physical time scale is much smaller

than  $x_r/u_r$ . The dimensionless form of (6) is the same as (6), except for the momentum equation, which becomes

$$m_t + (um)_x + \frac{p_r}{\rho_r u_r^2} p_x = 0 . \quad (7)$$

In compressible fluid dynamics it is customary and reasonable to choose for the unit  $p_r$  a value that is representative for the magnitude of the pressure in the flow, and similarly for  $\rho_r$ . As a consequence,  $c_r = \sqrt{\gamma p_r / \rho_r}$  is representative for the magnitude of the sound speed in the flow. We rewrite (7) as

$$m_t + (um)_x + \frac{1}{\gamma M_r^2} p_x = 0 , \quad M_r = u_r / c_r , \quad (8)$$

where  $M_r$  is representative for the values of the Mach number that actually occur. The fact that (8) is singular as  $M \downarrow 0$  is another indication of difficulties to be expected when standard methods for compressible flow are applied to weakly compressible flow.

Useful insight is gained by studying the asymptotic behaviour of the solution as  $M_r \downarrow 0$ . We consider the three-dimensional nonconservative version of the above equations:

$$\frac{D\rho}{Dt} + \rho \operatorname{div} \mathbf{u} = 0 , \quad (9)$$

$$\rho \frac{D\mathbf{u}}{Dt} + \frac{1}{\varepsilon} \operatorname{grad} p = 0 , \quad \varepsilon = \gamma M_r^2 , \quad (10)$$

$$\frac{Dp}{Dt} + \gamma p \operatorname{div} \mathbf{u} = 0 . \quad (11)$$

We postulate an asymptotic expansion of the following form:

$$\rho(t, \mathbf{x}) = \rho_0(t, \mathbf{x}) + \varepsilon \rho_1(t, \mathbf{x}) + \mathcal{O}(\varepsilon^2) ,$$

and similarly for the other two unknowns. To leading order, (10) gives  $\operatorname{grad} p_0 = 0$ , hence  $p_0 = p_0(t)$ . Equation (11) gives

$$\frac{1}{\gamma} \frac{d \ln p_0}{dt} = -\operatorname{div} \mathbf{u}_0 . \quad (12)$$

Integration over the flow domain  $\Omega$  gives

$$\frac{d \ln p_0}{dt} = -\frac{\gamma}{|\Omega|} \int_{\partial\Omega} \mathbf{u}_0 \cdot \mathbf{n} dS .$$

If the normal velocity is not prescribed along the whole boundary,  $p_0(t)$  must be given, otherwise it follows from (12). Hence,  $p_0(t)$  is known. Because  $p_0$  does not depend on  $\mathbf{x}$  it has no dynamic effect. Equation (9) gives

$$\left(\frac{\partial}{\partial t} + \mathbf{u}_0 \cdot \nabla\right) \ln \rho_0 = \frac{1}{\gamma} \frac{d \ln p_0}{dt} .$$

Equation (10) gives

$$\rho_0 \frac{D\mathbf{u}_0}{Dt} + \text{grad} p_1 = 0 . \quad (13)$$

Equations (12)–(13) determine  $\mathbf{u}_0$ ,  $\rho_0$  and  $p_1$ ;  $p_1$  acts as a Lagrange multiplier to allow  $\mathbf{u}_0$  to satisfy the constraint (12). When  $p_0$  and  $\rho_0$  are constant we recover the familiar incompressible Euler equations. For  $\rho_0$ ,  $\mathbf{u}_0$ ,  $p_0$  we have obtained a well-posed problem, so that we may conclude that the assumed asymptotic expansion is correct.

Since

$$p(t, \mathbf{x}) = p_0(t) + \varepsilon p_1(t, \mathbf{x}) + \mathcal{O}(\varepsilon^2) ,$$

there is for  $\varepsilon \ll 1$  a danger of rounding errors in numerical approximations of  $\text{grad } p$ . This can be avoided by working with  $p - p_0$  instead of  $p$ . This is possible because, as argued above,  $p_0(t)$  can be determined a priori. From (13) we see that  $p_1$  is of the same size as  $\rho_0 \mathbf{u}_0 \cdot \mathbf{u}_0$ . Therefore a good choice for the dimensionless pressure is

$$p = \frac{\hat{p} - \hat{p}_0}{\hat{\rho}_r \hat{u}_r^2} , \quad (14)$$

where for clarity the hat symbol is used to denote dimensional quantities. The other unknowns are made dimensionless as before. We now assume there is no global compression or expansion, so that  $\hat{p}_0(t) = \text{constant}$ , and flow into or out of closed vessels is excluded. We choose  $\hat{p}_0 = R \hat{\rho}_r \hat{T}_r$ , with  $\hat{T}_r$  a reference temperature that is typical for the temperatures that occur in the problem. The dimensionless equation of state is

$$\rho = (1 + \gamma M_r^2 p) / T .$$

Hence, as  $M_r \downarrow 0$  the dependence of  $\rho$  on  $p$  disappears, eliminating acoustics, but  $\rho$  still varies with  $T$ . The dimensionless form of the nonconservative equations of motion (6) is found to be, in three dimensions,

$$\begin{aligned} \rho_t + \text{div} \mathbf{m} &= 0 , & \mathbf{m}_t + (u\mathbf{m})_x + (v\mathbf{m})_y + (w\mathbf{m})_z + \text{grad} p &= 0 , \\ M_r^2 \left\{ \frac{Dp}{Dt} + \gamma p \text{div} \mathbf{u} \right\} + \text{div} \mathbf{u} &= 0 . \end{aligned} \quad (15)$$

We see that now the system does not become singular as  $M_r \downarrow 0$ . Furthermore, as  $M_r \downarrow 0$  the pressure equation reduce to the familiar solenoidality constraint of incompressible flow. The dimensionless form of the conservative energy equation is found to be

$$\begin{aligned}
 (\rho E)_t + \operatorname{div}(\mathbf{m}H) &= 0 , \\
 E &= e + \frac{1}{2}\gamma(\gamma - 1)M_r^2|\mathbf{u}|^2 , \quad H = h + \frac{1}{2}\gamma(\gamma - 1)M_r^2|\mathbf{u}|^2 ,
 \end{aligned}$$

with the dimensionless internal energy and enthalpy defined as  $e = T$ ,  $h = \gamma T$ .

## 5 STAGGERED SCHEME

We now generalize the incompressible staggered scheme of [13] to the compressible case. This is also done in [11], [12], [15], [17], [24], [36], [47]. In these methods the singularity for  $M \downarrow 0$  is not removed, as we do by splitting the pressure according to (14). It is shown in [24] that the other methods give unnecessary shock smearing by updating velocity instead of momentum in the pressure-correction step. All methods quoted derive the pressure-correction equation from the mass conservation equation, whereas equation (15) suggests that it is more appropriate to derive it from (the pressure formulation of) the energy equation, which we will do.

One may also generalize incompressible colocated schemes to the compressible case. This is done in [7]. In the incompressible colocated case, measures are required to suppress spurious pressure oscillations. This is usually done with the pressure-weighted interpolation method of [33]. This implies a perturbation of the mass conservation equation. An explicit expression for this perturbation is given in [26]. It is to be expected that this artificial perturbation masks weak compressibility effects. We prefer to stick with the staggered scheme.

To explain the basic principles, it suffices to consider the one-dimensional case. A staggered grid is used, with velocity and momentum at nodes  $x_{j+1/2} = jh$  and pressure and density at nodes  $x_j = (j - 1/2)h$ , with  $h$  the mesh size, assumed uniform. For higher order accuracy, we use the MUSCL slope-limited approach [48], [50] for spatial discretization and Runge-Kutta time stepping. These are familiar techniques in computational gasdynamics using colocated schemes, see for example [22]. These techniques are also used in the following scheme:

$$\begin{aligned}
 \rho_j^{(m+1)} - \rho_j^n + \alpha_{m+1}\lambda(u^{(m)}\rho^{(m)})|_{j-1/2}^{j+1/2} &= 0 , \quad \lambda = \tau/h , \\
 m_{j+1/2}^{(m+1)} - m_{j+1/2}^n + \alpha_{m+1}\lambda(u^{(m)}m^{(m)} + p^n)|_j^{j+1} &= 0 , \\
 \rho_j^{n+1} = \rho_j^{(4)} , \quad m_{j+1/2}^{n+1} = m_{j+1/2}^{(4)} - \frac{1}{2}\lambda\delta p|_j^{j+1} , \quad \delta p_j = p_j^{n+1} - p_j^n , \\
 M_r^2\{\delta p_j + \lambda(u^{n+1}p^n)|_{j-1/2}^{j+1/2} + \lambda(\gamma - 1)p_j^n u^{n+1}|_{j-1/2}^{j+1/2}\} + \lambda u^{n+1}|_{j-1/2}^{j+1/2} &= 0 .
 \end{aligned}$$

Here the superscript  $m \in \{0, 1, 2, 3\}$  is a Runge-Kutta stage counter. Following [38], we choose  $\alpha_1 = 1/4$ ,  $\alpha_2 = 1/3$ ,  $\alpha_3 = 1/2$ ,  $\alpha_4 = 1$ . The quantities  $\rho_{j+1/2}^{(m)}$ ,  $(u^{(m)}m^{(m)})_j$  and



$p_{j+1/2}^n$  are approximated with a slope-limited scheme, according to the MUSCL approach, for example, if  $u_{j+1/2}^{(m)} > 0$ :

$$\rho_{j+1/2}^{(m)} = \rho_j^{(m)} + \frac{1}{2}\psi(r_j)(\rho_{j+1}^{(m)} - \rho_j^{(m)}), \quad r_j = \frac{\rho_j^{(m)} - \rho_{j-1}^{(m)}}{\rho_{j+1}^{(m)} - \rho_j^{(m)}}.$$

For the limiter function we take the van Albada limiter ([44]). Substitution of  $u_{j+1/2}^{n+1} = (m/\rho)_{j+1/2}^{n+1}$  in the pressure equation gives for the pressure correction  $\delta p$  a linear system, that is reminiscent of a discretized convection-diffusion equation. Pressure correction is not included in the Runge-Kutta stages, to save computing time. Note that in the momentum equation the pressure is taken implicit (i.e.  $p^{n+1}$  is required for  $m^{n+1}$ ) and in the pressure equation the discrete approximation of  $\text{div}\mathbf{u}$  is taken at the new time. This is done in order to obtain a nonsingular discrete system for  $M_r = 0$ , that is identical to the classical incompressible pressure correction method of [13]. As a consequence, accuracy and efficiency equal those of incompressible methods as  $M_r \downarrow 0$ .

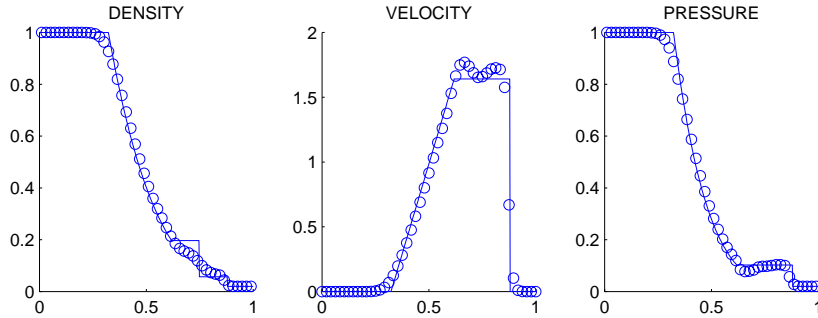


Figure 1: Solution of a Riemann problem;  $\lambda = 0.3$ ,  $h = 1/48$ ,  $t = 0.15$ .

The numerical solution of a Riemann problem is compared with the exact solution in Fig. 1. The maximum Mach number is 2. In this and similar problems the accuracy is found to be comparable to that of well-established colocated schemes, such as the Osher and AUSM schemes. Apparently, the staggered scheme satisfies the Rankine-Hugoniot and entropy conditions. Stationary contact discontinuities are found to be preserved. Extension to two dimensions is presented in [2]. How to formulate accurate staggered schemes on nonsmooth curvilinear two- and three-dimensional grids is discussed in [54], [53].

## 6 A NONCONVEX HYPERBOLIC SYSTEM

We will now consider the case of an arbitrary barotropic ( $p = p(\rho)$ ) equation of state, with application to hydrodynamic flow with cavitation in mind. The simplest nonlinear hyperbolic system is

$$V_t - u_y = 0, \quad u_t + p(V)_y = 0. \quad (16)$$

This is called the  $p$ -system. It describes one-dimensional flow of an inviscid barotropic medium in the Lagrange coordinate  $y$ , with  $V = 1/\rho$  the specific volume,  $u$  the velocity and  $p$  the pressure, satisfying the barotropic equation of state  $p = p(\rho)$ . The trajectory of a fluid particle that at  $t = 0$  is located at  $x = a$  is  $x = x(a, t)$ , and  $u = x_t$ . The Lagrange coordinate  $y$  is defined by  $y = \int \rho(a, 0) da$ . For completeness, we describe the transformation to Eulerian coordinates  $x, t = t$ . We have

$$\frac{\partial}{\partial y} = \frac{\partial x}{\partial y} \frac{\partial}{\partial x} = \frac{1}{\rho(a, 0)} \frac{\partial x}{\partial a} \frac{\partial}{\partial x}, \quad \frac{\partial}{\partial t} = \frac{\partial}{\partial \tilde{t}} + \frac{\partial x}{\partial \tilde{t}} \frac{\partial}{\partial x} = \frac{\partial}{\partial \tilde{t}} + u \frac{\partial}{\partial x}.$$

Mass conservation of a fluid particle requires that  $\rho(a, 0) da = \rho(x, t) = \rho(x(a, t), t) \frac{\partial x}{\partial a} da$ , so that  $\partial x / \partial a = \rho(a, 0) / \rho(x, t)$ . Substitution gives

$$\frac{\partial}{\partial y} = \frac{1}{\rho(x, t)} \frac{\partial}{\partial x}.$$

We see that transformation to the Eulerian frame gives the nonconservative barotropic Euler equations (deleting the tilde):

$$\rho_t + u\rho_x + \rho u_x = 0, \quad u_t + uu_x + \frac{1}{\rho} p_x = 0.$$

In order to explore some of the consequences of  $p(V)$  (or  $p(\rho)$ ) being nonconvex, we do some analysis on (16), rewritten as

$$U_t + f(U)_y = 0.$$

We recall a few basic facts; for more background, see [37]. The eigenvalues of the Jacobian  $f'(U)$  are  $\lambda_{1,2} = \mp C$ ,  $C^2 = -dp/dV$ . Assuming  $dp/dV < 0$ , we have a strictly hyperbolic system. The two members of (16) may be linearly combined as follows:  $u_t \pm CV_t \mp C(u_y - CV_y) = 0$ , and we see that the Riemann invariants are  $u \pm a$  with

$$a(p) = \int -C dV = \int \frac{1}{C} dp,$$

and that the characteristic curves satisfy  $dx/dt = \pm C$ . The jump condition at a shock is  $s[U] = [f]$ , so that the shock speed  $s$  satisfies  $s = \pm \sqrt{-[p]/[V]}$ , with  $[\cdot]$  the size of the jump. Physically relevant weak solutions must also satisfy the entropy condition: as time increases, characteristics must converge into shocks and may not emanate from shocks. We note that  $s^2$  corresponds to the slope of the chord connecting left and right shock states in the graph of  $p(V)$ , and the square of the characteristic velocity  $C^2$  corresponds to the slope of the tangent to the  $p(V)$  graph. A little reflection leads us to the formulation of the entropy condition due to Oleinik [27]:

*Right running waves must connect states following the upper concave hull of the  $p(V)$  graph, and left running waves must connect states following the lower convex hull of the  $p(V)$  graph.*

An example will follow.

For validation of numerical schemes in the absence of convergence theory, analytic solutions are helpful. Frequently, the Riemann problem for hyperbolic systems can be solved more or less explicitly. The domain is  $y \in \mathbb{R}$  and the initial conditions are given by

$$U(y, 0) = U_L, \quad y < 0; \quad U(y, 0) = U_R, \quad y > 0,$$

with  $U_{L,R}$  constant. If  $U(y, t)$  is a solution, then so is  $U(by, bt)$  with  $b$  an arbitrary positive constant. Hence, solutions may be sought in similarity form  $U(y, t) = U(\xi)$ ,  $\xi = y/t$ . Assuming a smooth solution, substitution gives  $(f' - \xi)U' = 0$ . Non-trivial solutions are obtained with

$$\xi = \lambda_{1,2}, \quad \frac{dU}{d\xi} = R_{1,2}, \quad R_{1,2} = (1, \pm C)^T,$$

where  $R_{1,2}$  are the eigenvectors of  $f'$ . Solutions of this type are called fans. For a left running fan,  $\xi = \lambda_1 = -C(\xi)$ . From  $U' = R_1$  we obtain:

$$0 = \frac{du}{d\xi} - C \frac{dV}{d\xi} = \frac{d(u+a)}{d\xi},$$

so that the Riemann invariant  $u + a = \text{constant}$  across left-running fans. Similarly,  $u - a = \text{constant}$  across right-running fans. Discontinuous similarity solutions are given by shocks:

$$U(\xi) = U_L, \quad \xi < s, \quad U(\xi) = U_R, \quad \xi > s.$$

Shocks and fans can be patched together to solve the Riemann problem; this is to be done such that the entropy condition is satisfied. How to do this in general is discussed in [52] and Chapt. 17 of [37]. Many possibilities have to be tested for a general equation of state and general  $U_{L,R}$ . We will simplify the situation such that a subclass of Riemann solutions is easily obtained. The equation of state is nonconvex with two inflection points, see Fig. 2. The symbols on the curve denote from right to left states 1 to 5; state 2 is indicated by a circle. The lower convex hull includes the tangent (not shown) to the graph between states 3 and 4. Note that  $p_3$  and  $p_4$  follow directly from the geometry of the  $p(V)$  graph, and can be determined a priori, which is the essence of our simplification. We assume that  $U_R = U_1$  and  $U_L = U_5$  are given such that the intermediate state  $U_2$  between right and left running waves satisfies  $V_2 > V_3$ . Then the structure of the

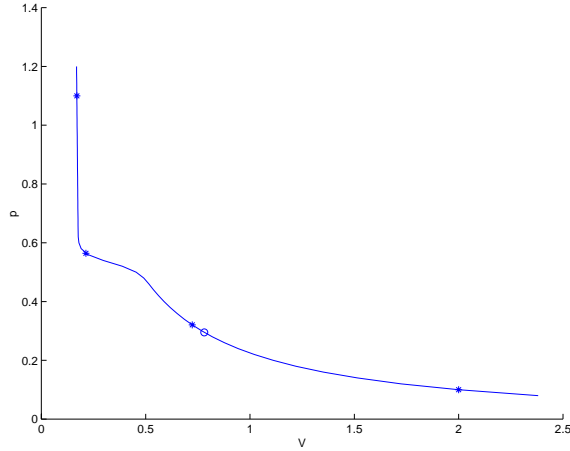


Figure 2: Graph of  $p(V)$  with assumed intermediate states in solution of Riemann problem.

solution follows from Oleinik's entropy condition. As noted before, in a fan the graph of  $p(V)$  is followed, and in a shock the chord between the left and right  $V$  is followed. Remembering that the solution must be on the upper concave hull for right running waves, a glance at Fig. 1 tells us that we must follow the chord between states 1 and 2. Hence, we have a shock between states 1 and 2. For left running waves the lower convex hull must be followed, so that we follow the tangent between states 3 and 4. Therefore we have a composite left running wave consisting of a fan between  $U_2$  and  $U_3$ , an expansion shock between  $U_3$  and  $U_4$ , and a fan between  $U_4$  and  $U_5$ . In the nonconvex case, the entropy condition does not forbid expansion shocks. If we succeed in finding a solution with the Ansatz implied by Fig. 2 we are done, otherwise more general methods must be followed. States 1 and 5 follow from the specification of the Riemann problem, and, as noted earlier,  $p_3$  and  $p_4$  follow from the geometry of the graph of  $p(V)$ . It remains to determine  $p_2$ ,  $u_2$ ,  $u_3$ ,  $u_4$ . We will derive an algebraic equation for  $p_2$ . For the shock between states 1 and 2 the jump condition gives:

$$u_2 = f_2(p_2) \equiv u_1 + (p_2 - p_1) / \sqrt{-(p_2 - p_1) / (V_2 - V_1)} .$$

For the left running fan between states 2 and 3 the Riemann invariant  $u + a$  is constant, so that

$$u_3 = f_3(p_2) \equiv f_2(p_2) + a(p_2) - a(p_3) .$$

For the left running shock between states 3 and 4 the speed  $s_{34}$  is known, because we know  $V_3$  and  $V_4$ . The jump condition gives

$$u_4 = f_4(p_2) \equiv f_3(p_2) + (p_4 - p_3) / s_{34} .$$

Finally, for the left running fan between states 4 and 5,  $u + a$  is constant, which gives

$$f_4(p_2) = u_5 + a_5 - a_4 .$$

If this equation has a real root the problem is solved.

The solution profile inside a fan is determined as follows. With practical applications in mind we switch to the Euler frame and use the conservation form of the barotropic Euler equations:

$$U_t + f(U)_x = 0 , \quad U = \begin{pmatrix} \rho \\ m \end{pmatrix} , \quad f = \begin{pmatrix} m \\ um + p(\rho) \end{pmatrix} . \quad (17)$$

In a similar way as before one finds that the characteristics and Riemann invariants are given by

$$\frac{dx}{dt} = u \pm c , \quad a \pm u = \text{constant} , \quad c = \sqrt{\frac{dp}{d\rho}} , \quad a = \int \frac{1}{\rho c} dp . \quad (18)$$

Postulating a similarity solution  $U = U(\xi)$ ,  $\xi = x/t$ , we find that for a left-running fan with  $\xi = \lambda_1 = u - c$  we have  $a + c + \xi = \text{constant}$ . This gives us  $p = p(\xi)$ , and  $u = u(\xi)$  follows from  $u = c + \xi$ . A right-running fan is handled similarly. Fig. 3 (drawn line) gives an example of a solution obtained in this way.

## 7 NUMERICAL METHODS FOR A NONCONVEX HYPERBOLIC SYSTEM

The linearized version of the  $p$ -system (16) is equivalent to the linearized shallow-water equations:

$$d_t + u_x = 0 , \quad u_t + g d_x = 0 , \quad (19)$$

with  $d$  the water depth, and  $g$  the acceleration of gravity. The average depth is unity. The shallow-water equations are usually discretized on a staggered grid, with depth nodes at  $x_j = (j - 1/2)h$  and velocity nodes at  $x_{j+1/2} = jh$ , with  $h$  the mesh size. This historic preference for a staggered grid for geophysical fluid dynamics and hydraulics goes back to the pioneering work of [34] on computation of atmospheric flows. Five different arrangements of nodes (including the colocated case) were studied systematically in [1], [32], with the grid used in [31] and [13] coming out best with respect to numerical dispersion and dissipation; this is the staggered grid also used here. The prevalence of colocated schemes in computational gasdynamics is to be ascribed to the fact that shock capturing is a more important issue than numerical dissipation and dispersion of smooth waves, and that staggered schemes are harder to implement accurately in two and three dimensions on nonsmooth curvilinear grids than colocated schemes; how this may be done is described in [54], [53].

The well-known schemes of [10], [21], [39], [40] for the full shallow-water equations are strongly related to the following staggered scheme for the one-dimensional linearized case (19) (Hansen scheme):

$$\begin{aligned} d_j^{n+1} - d_j^n + \lambda u^n |_{j-1/2}^{j+1/2} &= 0, \quad \lambda = \tau/h, \\ u_{j+1/2}^{n+1} - u_{j+1/2}^n + \lambda g d^{n+1/2} |_j^{j+1} &= 0, \quad d^{n+1/2} = (d^n + d^{n+1})/2. \end{aligned}$$

Because of its low computing cost and favorable dispersion and dissipation properties, we will apply a variation of the Hansen scheme to the nonconvex barotropic Euler equations. But first we will apply a colocated scheme, well-known in computational gasdynamics.

Most schemes in computational gasdynamics are specialized to the case of a perfect gas and need to be re-engineered for arbitrary equations of state, but the Osher scheme, [28], [29], is sufficiently general to make application to general equations of state straightforward. The scheme is colocated; all unknowns reside in the nodes  $x_j = (j - 1/2)h$ . Finite volume integration of (17) gives, putting  $j = 0$  for brevity,

$$U_0^{n+1} - U_0^n + \lambda(F_{1/2}^n - F_{-1/2}^n) = 0.$$

The numerical flux of the Osher scheme is

$$F_{1/2} = \frac{1}{2}\{f(U_0) + f(U_1)\} - \frac{1}{2} \int_{U_0}^{U_1} |f'(U)| dU.$$

The integral depends on the path chosen in state space between the states  $U_0$  and  $U_1$ . The path is parametrized by  $U = U(\sigma)$ ,  $0 \leq \sigma \leq 1$ ,  $U(0) = U_0$ ,  $U(1) = U_1$ , so that the integral becomes

$$\int_0^1 |f'(U)| \frac{dU}{d\sigma} d\sigma.$$

The integration path is chosen such that the integral is easy to evaluate and computing cost is small. The path is divided in two parts  $\Gamma_1$  ( $0 < \sigma < 1/2$ ) and  $\Gamma_2$  ( $1/2 < \sigma < 1$ ). The integration path is chosen such that

$$\frac{dU}{d\sigma} = R_2 \quad \text{on} \quad \Gamma_1, \quad \frac{dU}{d\sigma} = R_1 \quad \text{on} \quad \Gamma_2,$$

with  $R_{1,2}$  the eigenvectors of  $f'$ . This choice has the following consequences. Let  $R^1, R^2$  be row vectors such that  $R^\alpha R_\beta = \delta_\beta^\alpha$ . We have  $R_{1,2} = (1, u \mp c)^T$ ,  $R^{1,2} = (c \pm u, \mp 1)$ . Since

$$R^\alpha \frac{dU}{d\sigma} = 0 \quad \text{on } \Gamma_\alpha, \quad \alpha = 1, 2,$$

we find

$$0 = R^1 \frac{dU}{d\sigma} = \frac{1}{2c}(u+c) \frac{d\rho}{d\sigma} - \frac{1}{2c} \frac{d\rho u}{d\sigma} = \frac{1}{2} \frac{d\rho}{d\sigma} - \frac{\rho}{2c} \frac{du}{d\sigma}.$$

Equation (18) gives

$$\frac{da}{d\sigma} = \frac{1}{\rho c} \frac{d\rho}{d\sigma} = \frac{c}{\rho} \frac{d\rho}{d\sigma}.$$

We see that the Riemann invariant  $a - u$  is constant on  $\Gamma_1$ , so that  $(a - u)_{1/2} = (a - u)_0$ . Similarly,  $(a + u)_{1/2} = (a + u)_1$ . This gives us the state at  $\sigma = 1/2$ :

$$a_{1/2} = \frac{1}{2}(a_0 + a_1 + u_1 - u_0), \quad u_{1/2} = \frac{1}{2}(a_1 - a_0 + u_1 + u_0). \quad (20)$$

Next, we have to check whether  $\lambda_2 = u + c$  changes sign on  $\Gamma_1$ . This happens if  $(u_0 + c_0)(u_{1/2} + c_{1/2}) < 0$ . The sonic state on  $\Gamma_1$  (if any) is labeled with superscript  $s$  and subscript 1. In the sonic point we have

$$a_1^s + c_1^s = a_1^s - u_1^s = a_0 - u_0, \quad (21)$$

which can be solved for  $p_1^s$ . We have a sign change of  $\lambda_1 = u - c$  on  $\Gamma_2$  if  $(u_{1/2} - c_{1/2})(u_1 - c_1) < 0$ . In a similar way as before a sonic state on  $\Gamma_2$  follows from

$$a_2^s + s_2^s = a_1 + u_1. \quad (22)$$

The sonic value of  $\sigma$  on  $\Gamma_\alpha$  is called  $\sigma_\alpha$ . We can now evaluate the state space integral. We have

$$\begin{aligned} \int_0^{\sigma_1} |f'(U)| dU &= \int_0^{\sigma_1} |f'(U)| R_2 d\sigma = \int_0^{\sigma_1} |\lambda_2| R_2 d\sigma \\ &= \text{sign}(\lambda_2(0)) \int_0^{\sigma_1} \lambda_2 R_2 d\sigma = \text{sign}(\lambda_2(0)) \int_0^{\sigma_1} f'(U) R_2 d\sigma \\ &= \text{sign}(\lambda_2(0)) \int_0^{\sigma_1} f'(U) dU = \text{sign}(\lambda_2(0)) (f_{\sigma_1} - f_0). \end{aligned}$$

Similarly,

$$\int_{\sigma_1}^{1/2} |f'(U)| dU = \text{sign}(\lambda_2(\frac{1}{2}))(f_{1/2} - f_{\sigma_1}), \quad \int_{1/2}^{\sigma_2} |f'(U)| dU = \text{sign}(\lambda_1(1))(f_{\sigma_2} - f_{1/2}),$$

$$\int_{\sigma_2}^1 |f'(U)| dU = \text{sign}(\lambda_1(1))(f_1 - f_{\sigma_2}).$$

If there is no sonic point on  $\Gamma_1$  we get

$$\int_0^{1/2} |f'(U)| dU = \text{sign}(\lambda_2(\frac{1}{2}))f_{1/2} - \text{sign}(\lambda_2(0))f_0.$$

For the determination of  $U$  for  $\sigma = \sigma_1, 1/2, \sigma_2$  we have to solve the algebraic equations (20)–(22) for  $p$ . This involves the function  $a(p)$ , which must be computed by numerical quadrature for an arbitrary equation of state, so the Osher scheme is computationally expensive. But it gives satisfactory numerical results, as shown in Fig. 3.

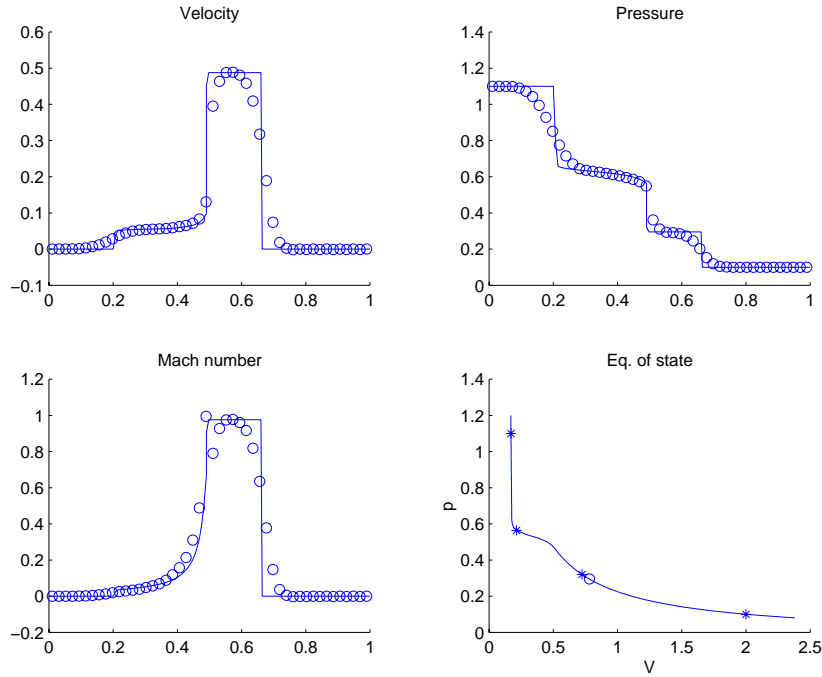


Figure 3: Solution of a Riemann problem with a nonconvex equation of state with the Osher scheme;  $t = 0.2, h = 1/48, \lambda = 0.4$ .

Because the scheme is only first order accurate the shock between states 1 and 2 is somewhat smeared, and the very steep expansion fan between states 4 and 5 is even more



smearred. Better accuracy can be obtained by using higher order flux-limited schemes for spatial discretization and Runge-Kutta time stepping, as discussed before.

Next, we apply the staggered scheme of Sect. 5, specialized to the barotropic case. The scheme is similar to the Hansen scheme, except that we take momentum implicit in the first equation, in order to obtain a unified method for compressible and incompressible flow. This time we use Euler time stepping and the first order upwind scheme in space. The resulting scheme is given by

$$\rho_j^{n+1} - \rho_j^n + \lambda m^{n+1}|_{j-1/2}^{j+1/2} = 0, \quad m_{j+1/2}^{n+1} - m_{j+1/2}^n + \lambda(u^n m^n + p^{n+1/2})|_j^{j+1} = 0, \quad (23)$$

where we use the first order upwind scheme:  $(u^n m^n)_{j+1} \cong (u^n m^n)_{j+1/2}$ . In one dimension, solving (23) takes little computing time, but in more dimensions this is expensive. We therefore use the pressure correction method, as in Sect. 5. First, a prediction for the momentum is made using the old pressure:

$$m_{j+1/2}^* - m_{j+1/2}^n + \lambda(u^n m^n + p^n)|_j^{j+1} = 0.$$

Next, a correction  $\delta m = m^{n+1} - m^*$  is postulated of the following form:

$$\delta m_{j+1/2} = -\frac{1}{2}\lambda\delta p|_j^{j+1}, \quad \delta p = p^{n+1} - p^n.$$

Substitution of  $m^{n+1} = m^* + \delta m$  in the mass conservation equation gives

$$\rho(p_j^{n+1}) - \rho(p_j^n) + \frac{1}{2}\lambda^2(\delta p|_{j-1}^j - \delta p|_j^{j+1}) = -\lambda m^*|_{j-1/2}^{j+1/2}. \quad (24)$$

This is a nonlinear equation for  $\delta p$ . Linearization gives

$$\rho_j^{n+1} - \rho_j^n \cong \left(\frac{d\rho}{dp}\right)_j^n \delta p_j = \delta p_j / (c_j^n)^2.$$

Substitution results in the following linear equation for the pressure correction:

$$\left(\frac{1}{c_j^n}\right)^2 \delta p_j + \frac{1}{2}\lambda^2(-\delta p_{j+1} + 2\delta p_j - \delta p_{j-1}) = -\lambda m^*|_{j-1/2}^{j+1/2}.$$

Results are shown in Fig. 4. The accuracy is the same as for the Osher scheme. But the staggered scheme requires much less computing time, because only simple central and upwind differences are used. Fig. 4 suggests that the staggered scheme converges to correct weak solutions.

An application in which the nonconvex barotropic Euler equations occur is the homogeneous equilibrium model for hydrodynamic flow with cavitation. A complete mathematical model with tracking of bubble interfaces is very computing intensive. A simplified approach is to adopt a hypothetical isothermal one-phase fluid with an artificial equation

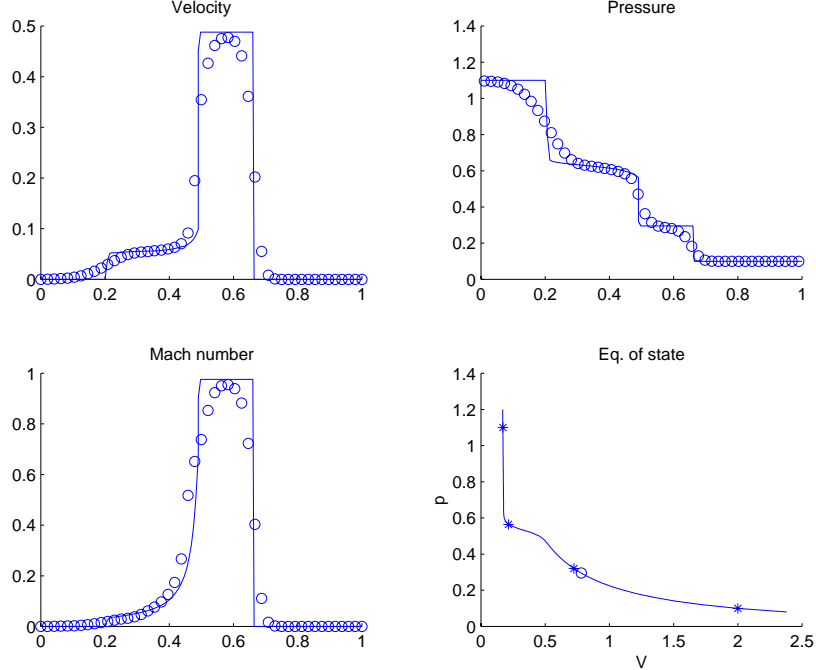


Figure 4: Solution of Riemann problem with staggered scheme;  $t = 0.2$ ,  $h = 1/48$ ,  $\lambda = 0.4$ .

of state  $p = p(\rho)$ , corresponding to water for  $p$  larger than a certain value  $p_2$ , and to vapor below a certain value  $p_1$ , with a smooth artificial transition for  $p_1 < p < p_2$ . This leads qualitatively to the kind of nonconvex equation of state shown in Fig. 2. This so-called homogeneous equilibrium model is used to compute flows with cavitation in [6], [14], [25], [45], [46].

In the wet part of the flow, the Mach number is very small, e.g.  $M \cong 10^{-3}$ . In the transition regime  $p_1 < p < p_2$  the speed of sound  $c = \sqrt{dp/d\rho}$  becomes very low, so that we have  $M$  as high as 25 in the application shown below. Therefore, to use the homogeneous equilibrium model as it stands, a unified compressible/incompressible numerical scheme is required that is efficient and accurate for both very low and very high Mach numbers. In some works, useful results have been obtained with numerical methods that do not satisfy this requirement, by modification of the homogeneous equilibrium model; for example, by making the water artificially compressible. Such a compromise is not needed with the present numerical method. Furthermore, the flows under consideration are usually unsteady, showing a cyclic shedding of bubbles. Therefore time accurate methods are called for. As seen in Sect. 3, this puts a burden on colocated schemes with low Mach preconditioning.

It turns out that the nonlinearity of  $p = p(\rho)$  is so strong that the linearized version pressure-correction equation (24) is not accurate enough, and that the nonlinear equation (23) must be solved iteratively to sufficient precision. Furthermore, to enhance stability

for high Mach numbers an upwind scheme needs to be used for  $\rho$  in the mass conservation equation, replacing  $m_{j+1/2}$  by  $u_{j+1/2}\rho_j$ ,  $u_{j+1/2} = 2m_{j+1/2}/(\rho_j + \rho_{j+1})$ . Higher order MUSCL type upwind approximations may also be used. To further enhance stability one may replace  $(um)^n$  by  $(um)^{n+1}$  in the momentum equation. These features, and stability analysis, are presented in [45], [46].

Fig. 5 shows a result concerning unsteady sheet cavitation in flow around the EN ([20]) hydrofoil. Darker shading corresponds to lower density. Cavitation bubbles are captured as regions of low density. There is good agreement with experimental observations.

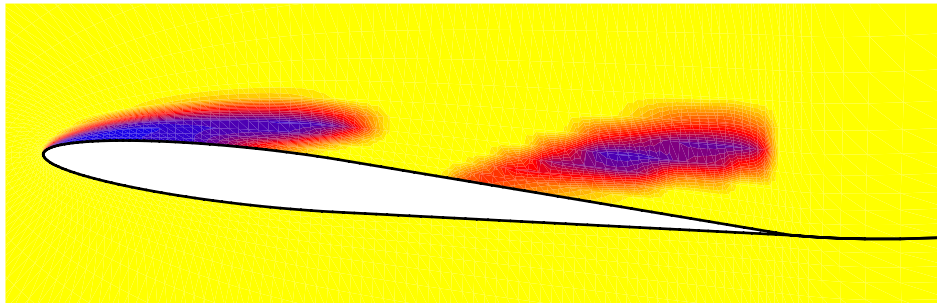


Figure 5: Density distribution in cavitating flow around EN hydrofoil, computed with homogeneous equilibrium model.

We conclude that staggered schemes provide a viable approach to unified compressible/incompressible methods for flows in which both very low and very high Mach numbers occur simultaneously.

## REFERENCES

- [1] A. Arakawa and V.R. Lamb, Computational design of the basic dynamical processes of the UCLA generalcirculation model. In J. Chang, editor, *Methods in Computational Physics*, volume 17, pages 173–265, New York, Academic Press, (1977).
- [2] H. Bijl and P. Wesseling, A unified method for computing incompressible and compressible flows in boundary-fitted coordinates, *J. Comp. Phys.*, **141**, 153–173, (1998).
- [3] D. Choi and C.L. Merkle, Application of time-iterative schemes to incompressible flow, *AIAA J.*, **23**, 1518–1524, (1985).
- [4] Y.-H. Choi and C.L. Merkle, The application of preconditioning in viscous flows, *J. Comp. Phys.*, **105**, 207–223, (1993).
- [5] D.L. Darmofal, Towards a robust multigrid algorithm with Mach number and i grid independent convergence. In K.D. Papailiou, D. Tsahalis, J. Périaux, and D. Knörzer, editors, *Computational Fluid Dynamics '98*, volume 2, pages 90–95, Chichester, Wiley, (1998).
- [6] Y. Dellanoy and J.L. Kueny, Two phase flow approach in unsteady cavitation modelling. In O. Furuya, editor, *Cavitation and Multiphase Flow Forum, Toronto, Ontario, Canada, June 4-7, 1990*, FED-98, pages 153–158, New York, ASME, (1990).
- [7] I. Demirdžić, Z. Lilek, and M. Perić, A collocated finite volume method for predicting flows at all speeds, *Int. J. Num. Meth. Fluids*, **16**, 1029–1050, (1993).
- [8] J.R. Edwards and C.J Roy, Preconditioned multigrid methods for two-dimensional combustion calculations at all speeds, *AIAA J.*, **36**, 185–192, (1998).
- [9] H. Guillard and C. Viozat, On the behavior of upwind schemes in the low Mach number limit, *Computers and Fluids*, **28**, 63–86, (1999).
- [10] W. Hansen, Theorie zur Errechnung des Wasserstandes und der Strömungen in Randmeeren nebst Anwendungen, *Tellus*, **8**, 289–300, (1956).
- [11] F.H. Harlow and A.A. Amsden, Numerical calculation of almost incompressible flows, *J. Comp. Phys.*, **3**, 80–93, (1968).
- [12] F.H. Harlow and A.A. Amsden, A numerical fluid dynamics calculation method for all flow speeds, *J. Comp. Phys.*, **8**, 197–213, (1971).
- [13] F.H. Harlow and J.E. Welch, Numerical calculation of time-dependent viscous incompressible flow of fluid with a free surface, *The Physics of Fluids*, **8**, 2182–2189, (1965).
- [14] H.W.M. Hoeijmakers, M.E. Janssens, and W. Kwan, Numerical simulation of sheet cavitation. In J.M. Michel and H. Kato, editors, *Third International Symposium on Cavitation, April 7–10, 1998, Grenoble*, volume 2, pages 257–262, (1998).
- [15] R. I. Issa, A. D. Gosman, and A. P. Watkins, The computation of compressible and incompressible flows by a non-iterative implicit scheme, *J. Comp. Phys.*, **62**, 66–82, (1986).
- [16] A. Jameson, W. Schmidt, and E. Turkel, Numerical solution of the Euler equations by finite volume methods using Runge-Kutta time stepping schemes. AIAA Paper 81-1259, (1981).

- 
- [17] K.C. Karki and S.V. Patankar, Pressure based calculation procedure for viscous flows at all speed in arbitrary configurations, *AIAA J.*, **27**, 1167–1174, (1989).
- [18] B. Koren, Improving Euler computations at low Mach numbers, *Int. J. Comp. Fluid. Dyn.*, **6**, 51–70, (1996).
- [19] B. Koren and B. van Leer, Analysis of preconditioning and multigrid for Euler flows with low-subsonic regions, *Advances in Comp. Meth.*, **4**, 127–144, (1995).
- [20] A. Kubota, H.Kato, H. Yamaguchi, and M. Maeda, Unsteady structure measurement of cloud cavitation on a foil section using conditional sampling technique, *J. Fluids Engrn*, **111**, 204–210, (1989).
- [21] J.J. Leendertse, *Aspects of a computational model for long period water-wave propagation*. PhD thesis, Delft University of Technology, (1967). Also appeared as Rand Memorandum RM-5294-PR, Rand Corporation, Santa Monica, California, 1967.
- [22] R.J. LeVeque, *Numerical methods for conservation laws*. Birkhäuser, Basel, (1992).
- [23] M.-S. Liou and C.J. Steffen, A new flux splitting scheme, *J. Comp. Phys.*, **107**, 23–39, (1993).
- [24] J.J. McGuirk and G.J. Page, Shock capturing using a pressure-correction method, *AIAA J.*, **28**, 1751–1757, (1990).
- [25] C.L. Merkle, J.Z. Feng, and P.E.O. Buelow, Computational modeling of the dynamics of sheet cavitation. In J.M. Michel and H. Kato, editors, *Third International Symposium on Cavitation, April 7–10, 1998, Grenoble*, volume 2, pages 307–311, (1998).
- [26] T.F. Miller and F.W. Schmidt, Use of a pressure-weighted interpolation method for the solution of the incompressible Navier-Stokes equations on a nonstaggered grid system, *Num. Heat Transfer*, **14**, 213–233, (1988).
- [27] O.A. Oleinik, Discontinuous solutions of nonlinear differential equations, *Uspekhi Mat. Nauk*, **12**, 3–73, (1957). (Amer. Math. Soc. Transl. Ser. 2, 26, pp. 95–172).
- [28] S. Osher, Numerical solution of singular perturbation problems and hyperbolic systems of conservation laws. In O. Axelsson, L.S. Frank, and A. van der Sluis, editors, *Analytical and numerical approaches to asymptotic problems in analysis*, pages 179–204, Amsterdam, North-Holland, (1981).
- [29] S. Osher and F. Solomon, Upwind difference schemes for hyperbolic systems of conservation laws, *Math. Comp.*, **38**, 339–374, (1982).
- [30] H. Paillère, S. Clerc, C. Viozat, I. Toumi, and J.-P. Magnaud, Numerical methods for low Mach number thermal-hydraulic flows. In K.D. Papailiou, D. Tsahalis, J. Périaux, and D. Knörzer, editors, *Computational Fluid Dynamics '98*, volume 2, pages 80–89, Chichester, Wiley, (1998i).
- [31] G.W. Platzman, A numerical computation of the surge of 26 June 1954 on Lake Michigan, *Geophysics*, **6**, 407–438, (1959).
- [32] D.A. Randall, Geostrophic adjustment and the finite difference shallow-water equations, *Monthly Weather Review*, **122**, 1371–1377, (1994).
- [33] C.M. Rhie and W.L. Chow, Numerical study of the turbulent flow past an airfoil with trailing edge separation, *AIAA J.*, **21**, 1525–1532, (1983).

- [34] L.F. Richardson, *Weather prediction by numerical process*. Cambridge Univ. Press, London, (1922). Reprinted, Dover, New York, 1965.
- [35] P.L. Roe, Approximate Riemann solvers, parameter vectors, and difference schemes, *J. Comp. Phys.*, **43**, 357–372, (1981).
- [36] W. Shyy and M.E. Braaten, Adaptive grid computation for inviscid compressible flows using a pressure correction method. AIAA Paper 88-3566-CP, (1988).
- [37] J. Smoller, *Shock waves and reaction-diffusion equations*. Springer-Verlag, New York, (1983).
- [38] B.P. Sommeijer, P.J. van der Houwen, and J. Kok, Time integration of three-dimensional numerical transport models, *Appl. Numer. Math.*, **16**, 201–225, (1994).
- [39] G.S. Stelling, *On the construction of computational methods for shallow water flow problems*. PhD thesis, Delft University of Technology, (1983). Also appeared as Rijkswaterstaat Communications 35, 1984. Rijkswaterstaat, The Hague.
- [40] G.S. Stelling, A.K. Wiersma, and J.B.T.M. Willemse, Practical aspects of accurate tidal computations, *J. Hydr. Eng.*, **112**, 802–817, (1986).
- [41] E. Turkel, Review of preconditioning techniques for fluid dynamics, *Appl. Num. Math.*, **12**, 257–284, (1993).
- [42] E. Turkel, A. Fiterman, and B. van Leer, Preconditioning and the limit of the compressible to the incompressible flow equations for finite difference schemes. In D.A. Caughey and M.M. Hafez, editors, *Frontiers of Computational Fluid Dynamics*, pages 215–234, Chichester, Wiley, (1994).
- [43] E. Turkel, R. Radespiel, and H. Kroll, Assessment of preconditioning methods for multidimensional aerodynamics, *Computers and Fluids*, **26**, 613–634, (1997).
- [44] G.D. van Albada, B. van Leer, and W.W. Roberts, A comparative study of computational methods in cosmic gas dynamics, *Astron. Astrophys.*, **108**, 76–84, (1982).
- [45] D.R. van der Heul, C. Vuik, and P. Wesseling, A staggered scheme for hyperbolic conservation laws applied to unsteady sheet cavitation, *Computing and Visualization in Science*, **2**, 63–68, (1999).
- [46] D.R. van der Heul, C. Vuik, and P. Wesseling, Segregated solution methods for compressible flow. *These proceedings*.
- [47] J.P. Van Doormaal, G.D. Raithby, and B.H. McDonald, The segregated approach to predicting viscous compressible fluid flows, *Transactions of the ASME - J. of Turbomachinery*, **109**, 268–277, (1987).
- [48] B. van Leer, Towards the ultimate conservative difference scheme. V. A second-order sequel to Godunov’s method, *J. Comput. Phys.*, **32**, 101–136, (1979).
- [49] B. Van Leer, Flux-vector splitting for the Euler equations. In E. Krause, editor, *Eighth International Conference on Numerical Methods in Fluid Dynamics*, pages 507–512, Berlin, Springer-Verlag, (1982). Lecture Notes in Physics 170.
- [50] B. van Leer, On the relation between the upwind-differencing schemes of Godunov, Enquist-Osher and Roe, *SIAM J. Sci. Stat. Comp.*, **5**, 1–20, (1984).

- [51] J.M. Weiss and W.A. Smith, Preconditioning applied to variable and constant density flows, *AIAA J.*, **33**, 2050–2057, (1995).
- [52] B. Wendroff, The Riemann problem for material with nonconvex equation of state. I: Isentropic flow, *J. Math. Anal. Appl.*, **38**, 454–466, (1972).
- [53] P. Wesseling, A. Segal, and C.G.M. Kassels, Computing flows on general three-dimensional nonsmooth staggered grids, *J. Comp. Phys.*, **149**, 333–362, (1999).
- [54] P. Wesseling, A. Segal, C.G.M. Kassels, and H. Bijl, Computing flows on general two-dimensional nonsmooth staggered grids, *J. Eng. Math.*, **34**, 21–44, (1998).